

Comparative Evolution of Jupiter and Saturn

W. B. Hubbard¹, T. Guillot², M. S. Marley³, A. Burrows⁴, J. I. Lunine^{1,6}, and D. S. Saumon⁵

¹Lunar & Planetary Lab., The Univ. of Arizona, Tucson, AZ 85721-0092 USA

²Obs. de la Côte d'Azur, F-06304 Nice Cedex 4, France

³Dept. of Astronomy, New Mexico State Univ., Las Cruces, NM 88003-0001 USA

⁴Dept. of Astronomy, The Univ. of Arizona, Tucson, AZ 85721 USA

⁵Dept. of Physics & Astronomy, Vanderbilt Univ., Nashville, TN 37235 USA

⁶Reparto di Planetologia, CNR – Istituto di Astrofisica, 00133 Roma Italy

Manuscript submitted to

Planetary and Space Science

Manuscript version from 9 December 1998

Offset requests to:

W. B. Hubbard

Lunar & Planetary Lab.

Tucson, AZ 85721-0092

Send proofs to:

W. B. Hubbard

Lunar & Planetary Lab.

Tucson, AZ 85721-0092

Abstract

We present evolutionary sequences for Jupiter and Saturn, based on new nongray model atmospheres, which take into account the evolution of the solar luminosity and partitioning of dense components to deeper layers. The results are used to set limits on the extent to which possible interior phase separation of hydrogen and helium may have progressed in the two planets. When combined with static models constrained by the gravity field, our evolutionary calculations constrain the helium mass fraction in Jupiter to be between 0.20 and 0.27, relative to total hydrogen and helium. This is in agreement with the Galileo determination. The helium mass fraction in Saturn's atmosphere lies between 0.11 and 0.25, higher than the Voyager determination. Based on the discrepancy between the Galileo and Voyager results for Jupiter, and our models, we predict that Cassini measurements will yield a higher atmospheric helium mass fraction for Saturn relative to the Voyager value.

1 Introduction

The thermal evolution of Jupiter and Saturn is a long-standing problem which couples the transport properties of the atmosphere and interior of Jupiter/Saturn, the thermodynamics and phase diagram of the deep interior, and the effect of solar heating of the atmosphere. New perspectives on this problem have been provided by recent experiments on the metallization of hydrogen at high pressures (Collins et al., 1998), new results for the composition of the jovian atmosphere from the Galileo entry probe (von Zahn, Hunten, and Lehmacher, 1998), and recent work by our research group on the evolution of extrasolar giant planets and brown dwarfs (Burrows et al., 1997).

The thermal evolution of a giant planet with an isentropic or near-isentropic interior temperature distribution is parametrized in terms of a surface which relates the three variables T_{eff} , T_{10} , and g , where T_{eff} is the effective temperature at which the planet radiates its internally-derived and converted solar energy into space, T_{10} is the temperature at 10 bars pressure, which characterizes the isentrope in the outer layers of the planet (note that if the atmosphere is radiative at 10 bars, T_{10} represents the temperature on the deeper isentrope extrapolated to 10 bars), and g is the surface gravity. The surface is shown in Fig. 1.

Figure 1 illustrates that the theory of the evolution of Jupiter and Saturn can be subsumed within a larger study of giant planets and brown dwarfs. The principal difference between Jupiter and Saturn and more massive bodies is that the evolution of the former involves a possible phase separation of helium within the metallic-hydrogen interior, as shown in Fig. 2 (Stevenson and Salpeter, 1977).

Evolution models of Jupiter and Saturn (Saumon et al., 1992; Guillot et al., 1995) have so far assumed the planet to remain homogeneous in the hydrogen-helium phase. This is questionable in the case of Jupiter, and certainly wrong for Saturn.

In Fig. 2, the solid curves show present-day Jupiter and Saturn, while the dashed curves show evolving models at earlier epochs with homogeneous and solar H-He proportions. In a fully consistent treatment of helium separation, the partitioning of helium in the metallic-hydrogen core would be calculated in accordance with a model free energy for a mixture of metallic hydrogen and helium. This paper does not carry out such a treatment. Rather, we introduce two limiting versions of separation of helium from hydrogen, carried out in such a way that the essential conclusions can be applied to separation of any denser

component (e.g., ice or rock) from hydrogen.

The helium distribution in a Jupiter or Saturn model is characterized by Y , the helium mass fraction of the hydrogen-helium mixture in a given layer. The hydrogen mass fraction is then $X = 1 - Y$. We characterize the value of Y in initial models with homogeneous hydrogen-helium composition by $Y_{\text{proto}} = 0.27$, which we take to be the initial protosolar value.

In the first version of the theory, discussed in Section 2, unmixing is assumed to occur with a linear time dependence, with the denser component (nominally He) being depleted by a constant factor throughout the molecular envelope and enriched by a constant factor throughout the metallic-hydrogen interior. In the second version, discussed in Section 3, unmixing occurs only in the final stages of evolution of the planet, occurring between the last dashed-curve model and the solid-curve model of Fig. 2. In the second version, the denser component is removed uniformly from all hydrogen-rich layers and added to a dense core at the center of the planet.

We will argue in the conclusion that the two versions of chemical evolution set limits on the possible unmixing in the two planets, and hence, on the maximum helium depletion to be expected in the atmosphere.

2 A semi-analytical non-homogeneous evolution model

2.1 Derivation

We present an estimation of the delay in the cooling of the planets introduced by helium (or any other element) differentiation using a simple analytical model.

The following assumptions are used: (i) the planet is fully isentropic, has no core, and is solely made of hydrogen and helium. (ii) It is initially homogeneous, but a phase separation (or phase transition) occurs at a fractional mass $m_t(t)$ (note that m ranges from 0 at the center to 1 at the surface), which leads to the creation of an upper helium poor region (labelled I), and a deeper helium-rich region (labelled II). The compositional difference between the two regions is defined by the difference in their hydrogen mass fraction $\Delta X(t) = X_{\text{I}} - X_{\text{II}}$. Note that $\Delta X(t)$ is a monotonically increasing function of t and that $\Delta X(0) = 0$. (iii) The transition region between I and II is infinitely small, and any change in composition due either to the variations of m_t or of ΔX with time is instantaneously redistributed by convection, so that regions I and II remain homogeneous

and adiabatic. (iv) Finally, we assume that the energy released by the falling helium droplets all goes into intrinsic planetary luminosity. In fact, a small fraction (about 10% perhaps) is retained in the form of a higher internal temperature (Stevenson and Salpeter, 1977).

Following Hubbard's (1977) procedure, we derive the evolution time scale from the energy conservation equation, but splitting the time derivative of the specific entropy S in two parts: a homogeneous, and an inhomogeneous part:

$$\frac{L}{M} = \int -T \left[\left(\frac{\partial S}{\partial t} \right)_X + \frac{dX}{dt} \left(\frac{\partial S}{\partial X} \right)_t \right] dm. \quad (1)$$

Here m is the mass fraction variable, normalized to unity at the planet's surface.

We assume that the total specific entropy depends linearly on the mass mixing ratios of hydrogen and helium, respectively (thereby neglecting the small contribution due to the mixing entropy). This yields

$$\left(\frac{\partial S}{\partial X} \right)_t = S_H - S_{He} \equiv \delta S, \quad (2)$$

where S_H and S_{He} are the specific entropies of pure hydrogen and pure helium, respectively.

Furthermore, using mass conservation in the planet between instants t and $t + dt$ yields:

$$\frac{dX}{dt} = \begin{cases} \Delta X \frac{dm_t}{dt} + m_t \frac{d\Delta X}{dt} & \text{if } m > m_t(t), \\ \Delta X \frac{dm_t}{dt} - (1 - m_t) \frac{d\Delta X}{dt} & \text{if } m < m_t(t + dt). \end{cases} \quad (3)$$

In this case, we assumed $m_t(t)$ to be a decreasing function of time (such as the plasma phase transition, which moves with time towards the center of the planet). This has no consequence on the final result however. The derivative dX/dt is infinite between $m_t(t)$ and $m_t(t + dt)$, but its integral over this mass interval is finite:

$$\int_{m_t(t+dt)}^{m_t(t)} -\frac{dX}{dt} T \delta S dm = T(m_t) \delta S(m_t) \Delta X \frac{dm_t}{dt} \quad (4)$$

Putting Eqs. 2, 3 and 4 into Eq.1 yields:

$$\begin{aligned} \frac{L}{M} = & \int -T \left(\frac{\partial S}{\partial t} \right)_X dm \\ & + \frac{d\Delta X}{dt} \left\{ \int_0^{m_t} T \delta S dm - m_t \int T \delta S dm \right\} \\ & - \Delta X \frac{dm_t}{dt} \left\{ \int T \delta S dm - T(m_t) \delta S(m_t) \right\} \end{aligned} \quad (5)$$

The first term on the right hand side of the equation corresponds to homogeneous contraction and cooling of the planet. The second one, proportional to $d\Delta X/dt$, is due to helium sedimentation. In our case, ΔX is monotonically increasing with time. Moreover, $T(m < m_t) > T(m > m_t)$ and $S(m < m_t) \sim S(m > m_t)$ (except in very particular cases which are of little importance here), so that this second term is positive. Helium sedimentation thus provides an additional energy source.

Finally, the third term, proportional to dm_t/dt , is caused by the displacement of the phase separation level with time. Its sign is unknown: if the transition between regions I and II follows the plasma phase transition (Saumon, Chabrier, and Van Horn, 1995), then m_t should decrease with time. On the other hand, a more general phase diagram could lead to either positive or negative dm_t/dt . Finally the bracketed term is generally negative, but only if m_t is not too close to the center of the planet (more than ~ 0.45). If this is verified, the whole third term is positive (i.e. provides energy) if the transition moves towards the planetary center, and negative if m_t gets closer to the surface.

2.2 Numerical application

We estimate quantitatively the significance of the different terms constituting Eq. 5 using today's models of Jupiter and Saturn. A more satisfactory approach would be the direct derivation of the equation and the calculation of an evolution consistently taking into account non-homogeneous effects. However, our simple approach is justified, in view of the uncertainties that remain on the hydrogen-helium phase diagram [Klepeis et al. (1991), Pfaffenzeller et al. (1995); see Guillot et al. (1995) for a discussion] or on the presence of a first order molecular/metallic hydrogen phase transition.

We assume that the phase separation level is closely associated to the molecular/metallic hydrogen transition and accordingly use the derivation by Saumon, Chabrier, and Van Horn (1995) to predict the value of m_t and its evolution with time. Its present value is ~ 0.85 in Jupiter and ~ 0.5 in Saturn. This number can change depending on the model, especially in the case of Saturn.

Thus, we find:

$$\int_0^{m_t} T\delta S dm - m_t \int T\delta S dm \simeq \begin{cases} 5 \times 10^{11} \text{ erg g}^{-1} & \text{for Jupiter} \\ 4 \times 10^{11} \text{ erg g}^{-1} & \text{for Saturn} \end{cases} \quad (6)$$

$$\int T\delta S dm - T(m_t)\delta S(m_t) \simeq \begin{cases} 2.5 \times 10^{12} \text{ erg g}^{-1} & \text{for Jupiter} \\ 10^{11} \text{ erg g}^{-1} & \text{for Saturn} \end{cases} \quad (7)$$

Furthermore, using homogeneous evolution calculations, we derive an upper limit to the displacement of the transition with time:

$$\left| \frac{dm_t}{dt} \right| < 2 \times 10^{-2} \text{ Gyr}^{-1}, \quad (8)$$

this relation being valid for Jupiter and Saturn. We can derive only an upper limit because any helium differentiation tends to slow the cooling and contraction of the planet.

These numerical estimations can be put into Eq. 5 and compared to the intrinsic luminosity per unit mass of Jupiter and Saturn, 5.7×10^{10} and $4.7 \times 10^{10} \text{ erg g}^{-1} \text{ Gyr}^{-1}$, respectively. Static interior models in agreement with the measured gravitational moments predict that $\Delta X < 0.08$ in Jupiter and that $0 < \Delta X < 0.60$ in Saturn. The contribution due to the displacement of the transition level is of the order of $5 \times 10^{10} \Delta X$ and $2 \times 10^9 \Delta X \text{ erg g}^{-1} \text{ Gyr}^{-1}$ in Jupiter and Saturn, respectively. It will therefore be neglected in this section. The following section presents an approximate treatment based on the phase diagram of Saumon, Chabrier, and Van Horn (1995). In general, this effect may contribute as much as $\sim 5\%$ change to the calculated ages.

The term proportional to dm_t/dt being thus ignored in Eq. 5, we derive the time delay due to a linear increase of the mass fraction discontinuity ΔX over the time Δt , by assuming that today's luminosity is entirely due to the differentiation:

$$\Delta t \simeq \begin{cases} 9.1 \Delta X \text{ Gyr} & \text{for Jupiter,} \\ 8.3 \Delta X \text{ Gyr} & \text{for Saturn.} \end{cases} \quad (9)$$

Using model ages from homogeneous evolution calculations, and reasonable uncertainties due to both the model atmospheres and to the approximations inherent in our semi-analytical model, we can hence constrain ΔX .

For Jupiter, calculations based on homogeneous evolution (see below) give model ages between 3.6 and 5.1 Gyr, the lower limit being derived from models with a radiative zone and an interpolated equation of state, and the upper limit from fully adiabatic models with a PPT EOS. With a ~ 0.3 Gyr uncertainty, we derive that, for Jupiter, $-0.09 < \Delta X < 0.12$. This global constraint is not very useful and has in fact to be linked to the various static models to predict values of ΔX . In the case of Saturn, homogeneous evolution models predict ages between 2 and 3 Gyr. It therefore appears that a more useful constraint can be derived for this planet: $0.15 < \Delta X < 0.34$.

3 Core formation model

3.1 Helium differentiation

In this section we present an alternative approach in which we estimate the heat evolved during a single time step δt in which a dense component settles out from a hydrogen-helium mixture into the core. The dense component is taken to be helium, but similar considerations apply to any constituent whose specific entropy is much smaller than hydrogen's (as is true in general). Thus we write a variant of Eq. 1 in the following form:

$$\delta t = - \left[\int dm T \delta S \right] / (L/M), \quad (10)$$

where

$$L = 4\pi R^2 \sigma (T_{\text{eff}}^4 - T_S^4), \quad (11)$$

with R the radius of the planet's photosphere and T_S the effective radiating temperature that the photosphere would have if it were radiating only thermalized sunlight. For homogeneous evolution, T_{eff} and specific entropy S (as parametrized by T_{10}) are uniquely related at each point in the evolution, via the surface presented in Fig. 1. We treat inhomogeneous evolution by starting with an optimized model of present Jupiter or Saturn with specified helium mass fraction (relative to the total hydrogen-helium mass) Y in the entire hydrogen-rich portion of the planet. The remaining helium or other dense component is assumed to be incorporated in a central core. In some sense, this model represents an upper limit on the heat release (and concomitant prolongation of cooling) caused by a given amount of helium separation, since the mass of low-specific-entropy material displaced to the center of the planet is maximized.

We now consider evolution backward in time to a previous model in which the helium incorporated in the core is restored to the hydrogen-rich envelope, which then has a helium mass fraction equal to $Y = Y_{\text{proto}} = 0.27$. The time step involved in this process is evaluated using Eq. (10). At prior times the evolution is homogeneous.

In the sample calculations presented here, we assume, for Jupiter, that the planet evolves from a uniform $Y = 0.27$ to a separated model at present with $Y = 0.24$ in the entire H part of the planet and pure He (corresponding to the depleted amount of He) in a core at the center. For Saturn, we assume the same scenario except that the present model has $Y = 0.20$ in the entire H part of the planet.

For both planets, the following effects occur between the present-day model (shown with solid line in Fig. 2) and the previous undifferentiated model. First, the central temperature is *larger* in the present-day model because of greater differentiation. This corresponds to the energy retained in the form of a higher internal temperature mentioned previously. Second, a mass element which is depleted in the denser component (going forward in time) goes to a higher specific entropy, because it is richer in H, while mass elements near the center of the planet go to a lower specific entropy. Because the latter are at a higher temperature than the former, there is a net heat release going forward in time. The heat which is released to space during this single time step, i.e. total heat release less heat stored via heating of the interior due to core formation, is $1.9 \times 10^{11} \text{ erg g}^{-1}$ for Jupiter, and $1.8 \times 10^{11} \text{ erg g}^{-1}$ for Saturn. Similar values are found from Eqs. (5) and (6), when assuming $\Delta X \sim 0.8$ and $m_t \sim 0.04$ for Jupiter and $m_t \sim 0.09$ for Saturn (where in this case m_t denotes the mass fraction of the pure helium core).

3.2 Variable and constant solar heating

Figure 3 shows the evolution of Jupiter and Saturn for three assumptions about solar heating. The crosses show the evolution of isolated objects with $T_S = 0$. The open circles show evolution with T_S held constant at its present value for each planet, while the dots show evolution with a variable T_S computed on the assumption that the solar luminosity has increased roughly linearly with time from an initial value of about 72% of the present luminosity.

This calculation assumes that Jupiter’s Bond albedo has remained constant in time at its present value (0.343). However it is likely that during the time water clouds first condensed in the planet’s atmosphere (near $T_{\text{eff}} = 400$ K), the Bond albedo was substantially higher for a time until the clouds moved lower in the atmosphere with decreasing T_{eff} . At earlier times still the planet would be free of clouds of abundant species, yet the Bond albedo would be similar to the current time. Marley et al. (1999) discuss Bond albedos for Jupiter-like models with and without clouds.

Figure 4 shows an expanded view of the final stages of evolution of Jupiter and Saturn. The vertical error bars show the present values for the two planets. The heavy horizontal error bar shows the prolongation of ages for the $Y_{\text{proto}}-Y$ assumed in this section. However, it assumes the linear differentiation with time of the previous section, and that the helium separates into the metallic hydrogen region but not the very center of the planet.

4 Summary

Our conclusions are as follows.

(a) The atmospheric boundary conditions are reasonably well understood (see Fig. 1) and are no longer a source of major uncertainty in the cooling theory for Jupiter and Saturn. With these boundary conditions and the assumption of homogeneous evolution, Jupiter cools to its present T_{eff} in 3.6 to 5.2 Gyr, while Saturn cools to its present T_{eff} in approximately 2 to 3 Gyr. Therefore differentiation is needed to account for Saturn’s present luminosity, but not necessarily for Jupiter’s.

(b) Solar heating prolongs the cooling time of Jupiter by about 1 Gyr and the cooling time of Saturn by about 0.5 Gyr. Allowance for lower solar heating in the past reduces the effect by ~ 0.1 Gyr for both planets, a very minor effect. Likewise variation in the planetary Bond albedo with time will have comparably small effects on the evolution.

(c) We have considered two limiting models for He differentiation in Jupiter. The model presented in Section 3 shows that a pure helium core cannot have formed in Jupiter and result in the presently observed atmospheric Y . Such a recent differentiation in Jupiter, corresponding to a reduction of the atmospheric Y by about 0.03 (the Voyager result) would indeed prolong the evolution by about another 2 Gyr. In contrast, the model presented in Section 2 predicts that the difference between the primordial helium mass fraction Y_{proto} and the present atmospheric Y should lie in the range $-0.08 < Y_{\text{proto}} - Y < 0.10$. Note that a value of zero for $Y_{\text{proto}} - Y$ corresponds to no differentiation, whereas a negative value indicates an unlikely upward transport of any element other than hydrogen. However models for which $Y_{\text{proto}} - Y > 0.07$ cannot reproduce the planet's gravitational field (Guillot, 1999). Thus $0.20 < Y < 0.27$. This is higher than the Voyager value $Y = 0.18$ (Gautier and Owen, 1989) but it includes the new Galileo value $Y = 0.238$ (von Zahn, Hunten, and Lehmacher, 1998).

(d) We have considered two limiting models for He differentiation in Saturn. The model presented in Section 3 shows that recent differentiation of helium in Saturn, corresponding to a reduction of the atmospheric Y by about 0.07 would prolong the evolution by about another 2 Gyr, bringing agreement between the observed age and T_{eff} . The model presented in Section 2 predicts that $0.06 < Y_{\text{proto}} - Y < 0.14$, and hence $0.13 < Y < 0.21$. Neither limiting model includes the Voyager value $Y = 0.06 \pm 0.05$. The case for a higher atmospheric Y in Saturn is further strengthened by static models, the enrichment in heavy elements required to fit the planetary gravitational field being incompatible with the observed methane abundance for $Y < 0.11$ (Guillot, 1999).

(e) The models presented must both be corrected for the fact that the energy that results from differentiation is not added entirely at the end of the evolution. Should helium differentiation occur very early in the evolution (a very unlikely assumption), the subsequent time delay would be negligible compared to the present calculations. In most likely cases, we estimate that it yields time delays overestimated by $\sim 5\%$ for Jupiter, and by $\sim 10 - 30\%$ for Saturn.

(f) The most precise determination of the Jovian helium abundance in the outer atmosphere is that of the Galileo Helium Abundance detector, and our results are in excellent agreement with that measurement. The Voyager-determined Jovian helium abundance lies below both, and indeed for Saturn we also predict a helium abundance larger than that determined by Voyager. Both the very precise Galileo HAD determination and that of the Galileo mass spectrometer (Niemann et al., 1998), which is fully consistent with but less precise than the HAD value, give us confidence in our model results. In fact, we suggest that a reexamination of the Voyager helium determinations for both planets may be order, specifically with the aim of assessing whether the initial analyses has errors that systematically lowered the helium abundances. This exercise is not an academic one, because the Cassini mission enroute to Saturn will not be capable of providing in situ measurements of the helium abundance. The Galileo Jupiter results combined with ours raise a potential concern that the Cassini remote sensing measurements to determine helium in Saturn, using CIRS and radio occultations, might be subject to similar systematic errors.

It must be stressed that these are still preliminary models. A more detailed study interfaced to a complete physical picture of the H-He phase diagram is in preparation. We should also note that in either limiting model, the extra heat which is liberated could come from the differentiation of some other dense component beside helium. Thus an observational result indicating a primordial solar value for the atmospheric helium abundance would not necessarily preclude extension of the cooling time via differentiation of another abundant component.

Acknowledgements. Research supported by the National Aeronautics and Space Administration (Origins Program), the National Science Foundation, and the “Groupe de Recherche Structure Interne des Etoiles et des Planètes Géantes”.

References

- Burrows, A., Marley, M., Hubbard, W. B., Lunine, J. I., Guillot, T., Saumon, D., Freedman, R., Sudarsky, D., and Sharp, C., A non-gray theory of extrasolar giant planets and brown dwarfs, *Astrophys. J.*, *491*, 856–875, 1997.
- Collins, G. W., Da Silva, L. B., Celliers, P., Gold, D. M., Foord, M. E., Wallace, R. J., Ng, A., Weber, S. V., Budil, K. S., and Cauble, R., Measurements of the equation of state of deuterium at the fluid insulator-metal transition, *Science*, *281*, 1178–1181, 1998.
- Gautier, D., and Owen, T., 1989. The composition of outer planet atmospheres. In: Atreya, S. K., Pollack, J. B., and Matthews, M. S. (Eds.), *Origin and Evolution of Planetary and Satellite Atmospheres*. The University of Arizona Press, Tucson, Arizona and London.
- Guillot, T., Chabrier, G., Gautier, D., and Morel, P., Effect of radiative transport on the evolution of Jupiter and Saturn, *Astrophys. J.*, *450*, 463–472, 1995.
- Guillot, T., A comparison of the interiors of Jupiter and Saturn, submitted to *Planet. Space Sci.*, 1999.
- Hubbard, W. B., The jovian surface condition and cooling rate, *Icarus*, *30*, 305–310, 1977.
- Hubbard, W. B., Guillot, T., Lunine, J. I., Burrows, A., Saumon, D., Marley, M. S., and Freedman, R. S., Liquid metallic hydrogen and the structure of brown dwarfs and giant planets, *Physics of Plasmas*, *4*, 2011–2015, 1997.
- Klepeis, J. E., Schafer, K. J., Barbee, T. W., III, and Ross, M., Hydrogen-helium mixtures at megabar pressures: Implications for Jupiter and Saturn, *Science*, *254*, 986–989, 1991.
- Marley, M. S., Gelino, C., Stephens, D., Lunine, J., and Freedman, R., Reflected spectra and albedos of extrasolar giant planets I: Clear and cloudy atmospheres, *Astrophys. J.*, *513*, in press, 1999.
- Niemann, H. B., Atreya, S. K., Carignan, G. R., Donahue, T. M., Haberman, J. A., Harpold, D. N., Hartle, R. E., Hunten, D. M., Kasprzak, W. T., Mahaffy, P. R., Owen, T. C., and Way, S. H., The composition of the Jovian atmosphere as determined by the Galileo probe mass spectrometer, *J. Geophys. Res.*, *103*, 22831–22845, 1998.
- Pfaffenzeller, O., Hohl, D., Ballone, P., Miscibility of hydrogen and helium under astrophysical conditions, *Phys. Rev. Lett.*, *74*, 2599–2602, 1995.
- Saumon, D., Chabrier, G., and Van Horn, H. M., An equation of state for low-mass stars and giant planets, *Astrophys. J. Suppl.*, *99*, 713–741, 1995.
- Saumon, D., Hubbard, W. B., Chabrier, G., and Van Horn, H. M., The role of the molecular-metallic transition of hydrogen in the evolution of Jupiter, Saturn, and brown dwarfs, *Astrophys. J.*, *391*, 827–831, 1992.
- Stevenson, D. J., and Salpeter, E. E., The dynamics and helium distribution properties for hydrogen-helium fluid planets, *Astrophys. J. Suppl.*, *35*, 239–261, 1977.
- von Zahn, U., Hunten, D. M., and Lehman, G., Helium in Jupiter’s atmosphere: Results from the Galileo probe helium interferometer experiment, *J. Geophys. Res.*, *103*, 22815–22829, 1998.

Figure Captions

Fig. 1. This surface is produced by a splined fit to individual model atmospheres (Burrows et al., 1997), augmented by additional unpublished calculations. Solid dots show non-gray calculations, while open circles show gray calculations. The superimposed trajectories show evolution for homogeneous isolated bodies with masses equal to (lower left to upper right) Saturn, Jupiter, 5 Jupiters, 10 Jupiters, and 42 Jupiters. Dotted lines show evolution at age $t < 10^8$ years, heavy dashed lines show evolution for t between 10^8 and 10^9 years, and solid lines show evolution at $t > 10^9$ years.

Fig. 2. Phase diagram of hydrogen (Hubbard et al., 1997), with evolution of Jupiter and Saturn. Bodies more massive than Jupiter will not enter the He rainout region within a Hubble time. The phase transition between liquid molecular hydrogen and liquid metallic hydrogen is according to the theory of Saumon, Chabrier, and Van Horn (1995).

Fig. 3. Variation of T_{eff} vs. t for homogeneous (solar-composition) Jupiter and Saturn; large dots show present values. The final time steps illustrate the effect of He differentiation and are shown in expanded scale in the next figure.

Fig. 4. Expanded view of the final stages of evolution of Jupiter and Saturn, assuming that He differentiation occurs in the final time step. Dashed curves show evolution without He differentiation. Heavy horizontal error bars show prolongation of evolution for the same atmospheric helium depletion assumed here, but using the theory of Section 2.

Figures

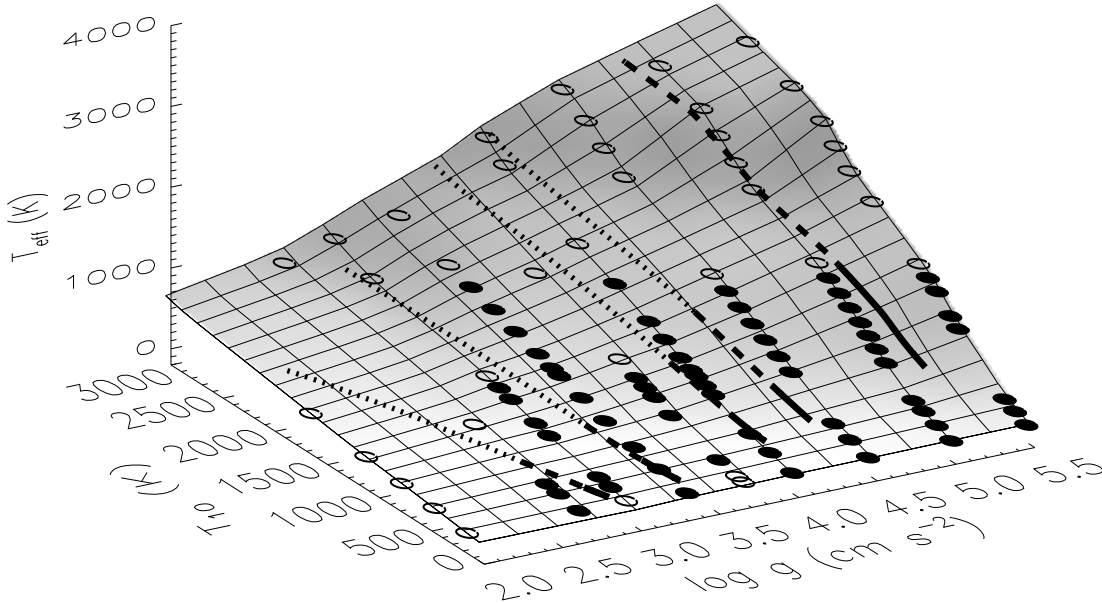


Fig. 1. This surface is produced by a splined fit to individual model atmospheres (Burrows et al., 1997), augmented by additional unpublished calculations. Solid dots show non-gray calculations, while open circles show gray calculations. The superimposed trajectories show evolution for homogeneous isolated bodies with masses equal to (lower left to upper right) Saturn, Jupiter, 5 Jupiters, 10 Jupiters, and 42 Jupiters. Dotted lines show evolution at age $t < 10^8$ years, heavy dashed lines show evolution for t between 10^8 and 10^9 years, and solid lines show evolution at $t > 10^9$ years.

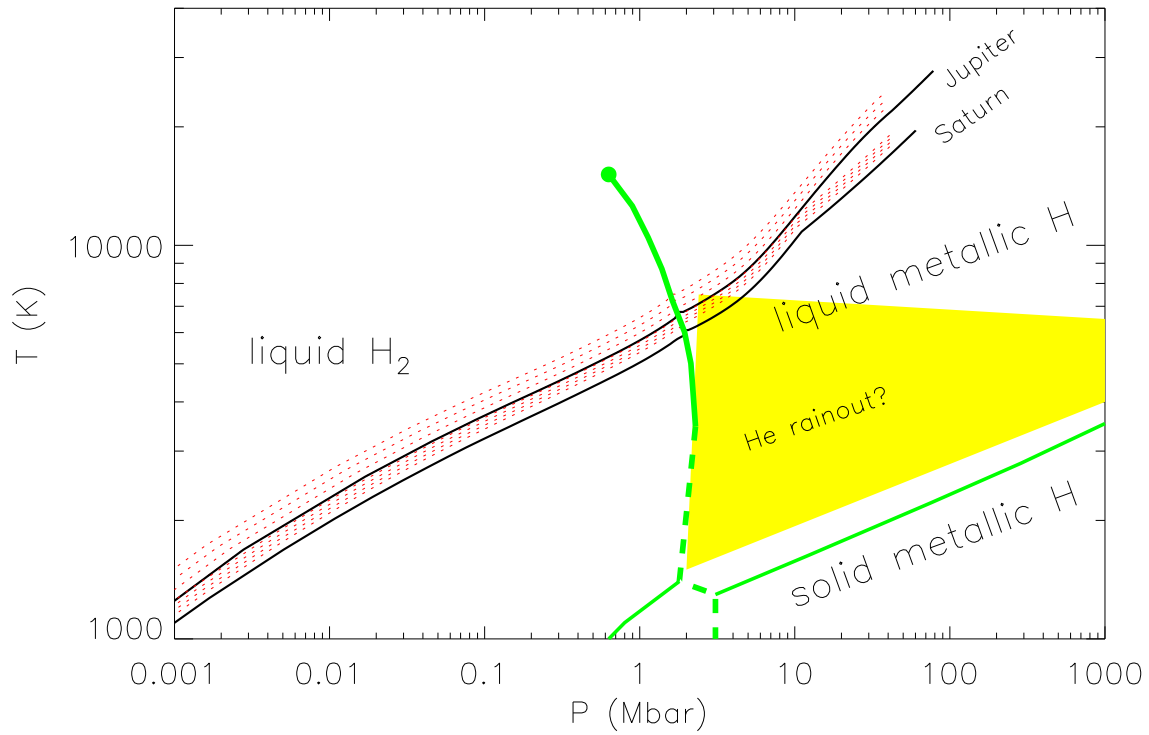


Fig. 2. Phase diagram of hydrogen (Hubbard et al., 1997), with evolution of Jupiter and Saturn. Bodies more massive than Jupiter will not enter the He rainout region within a Hubble time. The phase transition between liquid molecular hydrogen and liquid metallic hydrogen is according to the theory of Saumon, Chabrier, and Van Horn (1995).

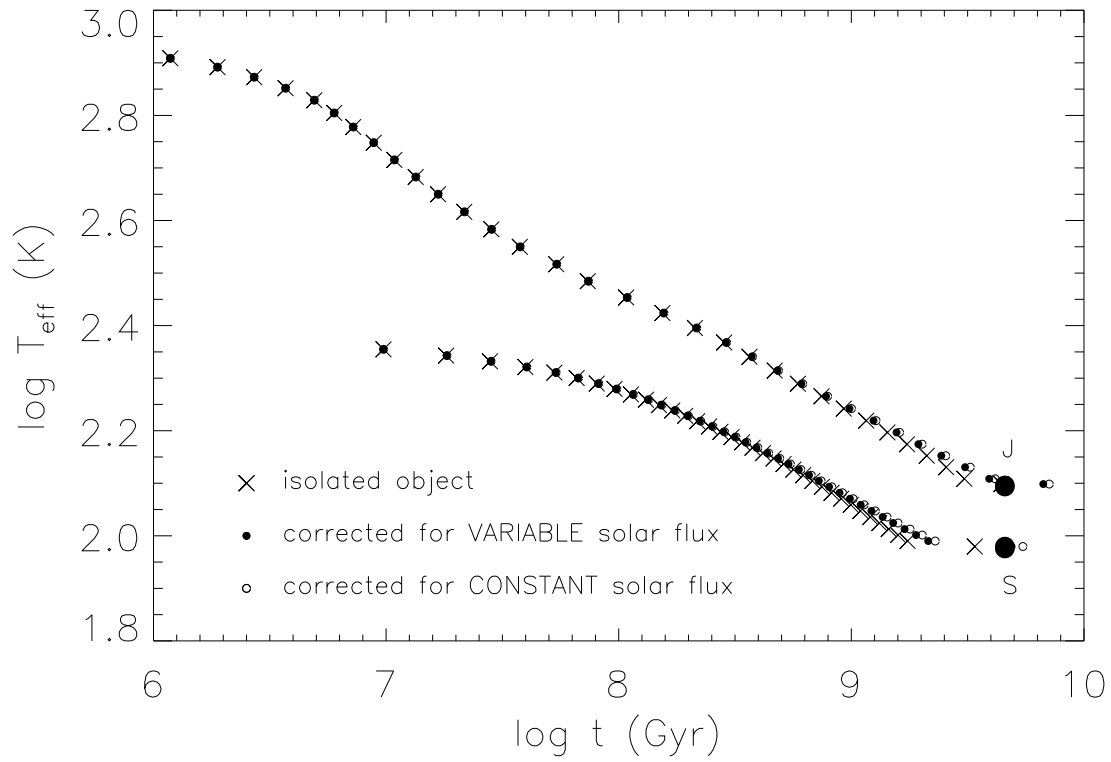


Fig. 3. Variation of T_{eff} vs. t for homogeneous (solar-composition) Jupiter and Saturn; large dots show present values. The final time steps illustrate the effect of He differentiation and are shown in expanded scale in the next figure.

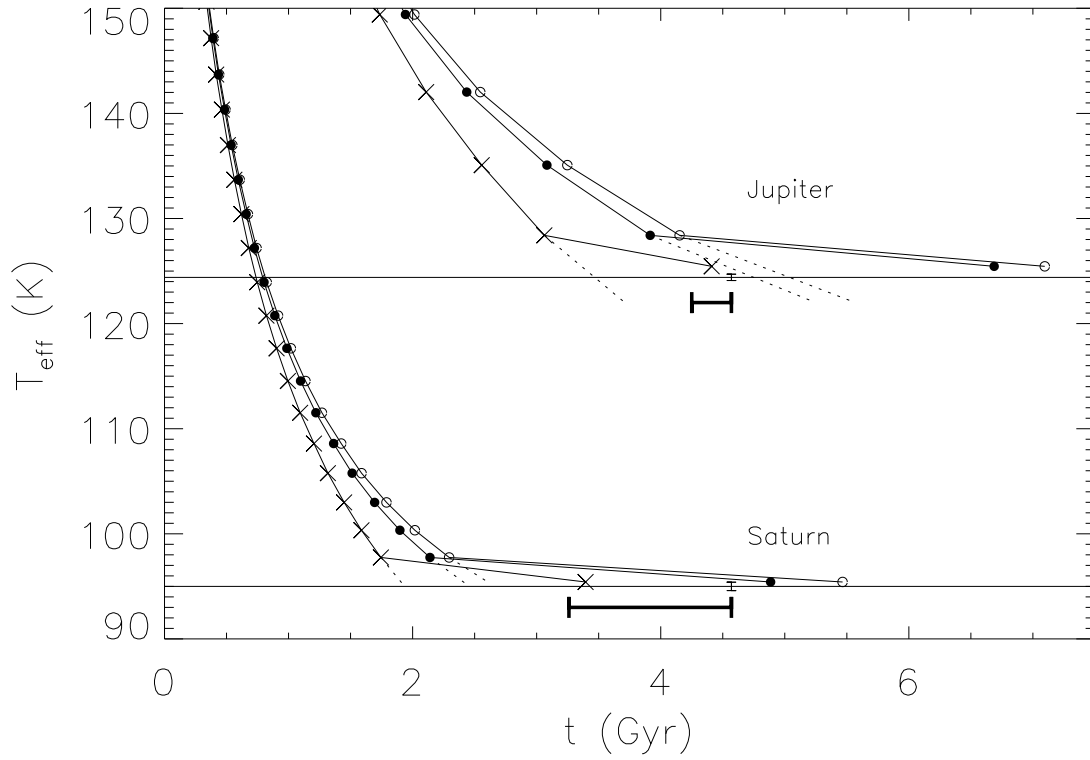


Fig. 4. Expanded view of the final stages of evolution of Jupiter and Saturn, assuming that He differentiation occurs in the final time step. Dashed curves show evolution without He differentiation. Heavy horizontal error bars show prolongation of evolution for the same atmospheric helium depletion assumed here, but using the theory of Section 2.